Clim. Past Discuss., 9, 4293–4322, 2013
www.clim-past-discuss.net/9/4293/2013/
doi:10.5194/cpd-9-4293-2013
© Author(s) 2013. CC Attribution 3.0 License.

Climate of the Past Discussions
Open Access

This discussion paper is/has been under review for the journal Climate of the Past (CP).
Please refer to the corresponding final paper in CP if available.

Reconstruction of Atlantic Water variability during the Holocene in the western Barents Sea

D. E. Groot, S. Aagaard-Sørensen, and K. Husum

Department of Geology, University of Tromsø, Tromsø, Norway

Received: 3 July 2013 – Accepted: 4 July 2013 – Published: 30 July 2013

Correspondence to: D. E. Groot (diane.e.groot@uit.no)

Published by Copernicus Publications on behalf of the European Geosciences Union.

Abstract

The gravity core JM09-KA11-GC from 345 m water depth on the western Barents Sea margin was investigated for distribution patterns of benthic foraminifera, stable isotopes, and sedimentological parameters to reconstruct the flow of Atlantic Water during the Holocene. The core site is located below the Atlantic water masses flowing into the Arctic Ocean and close to the Arctic Front. The results show continuous presence of Atlantic Water at the margin throughout the Holocene. During the Early Holocene, (11 700–9400 cal yr BP), bottom water temperatures rose by 2.5 °C due to the increased influence of Atlantic Water, although sea-ice was still present at this time. The transition to the Mid Holocene is characterized by a local shift in current regime, resulting in a ceased supply of fine-grained material to the core location. Throughout the Mid Holocene the $\delta^{18}O$ values indicate a slight cooling, thereby following changes in insolation. In the last 1500 yr, inflow of Atlantic Water increased but was interrupted by periods of increased influence of Arctic Water causing periodically colder and more unstable conditions.

1 Introduction

The climate in the European Arctic is strongly dependent on the inflow of warm and saline Atlantic Water masses transported to the high northern latitudes by the North Atlantic Current (NAC). Its most distal branch, the West Spitsbergen Current (WSC) is considered to be the major pathway for heat, salt, and water flux to the Arctic Ocean (e.g. Aagaard and Greisman, 1975).

Throughout the Holocene, the strength of Atlantic Water inflow into the northern North Atlantic has varied, although with smaller amplitude than is recorded for the glacial periods (e.g. Klitgaard-Kristensen et al., 2001; Risebrobakken et al., 2003; Hald et al., 2007). Several marine records covering the Holocene in the Barents Sea region have demonstrated that even small variations in the intensity of Atlantic Water inflow

CPD
9, 4293–4322, 2013

can have a strong impact on climate at the high northern latitudes (e.g. Duplessy et al., 2001; Lubinski et al., 2001; Sarnthein et al., 2003; Ślubowska-Woldengen et al., 2007). These studies indicate that short and long term climatic changes, such as the transition from the warm Early Holocene to the cool and stable Mid Holocene, are associated with changes in the flow of Atlantic Water and the oceanic conveyor belt in addition to changes in insolation forcing. Furthermore, variability of Atlantic Water influence can be attributed to more local factors such as the distribution of Polar Water (e.g. at the SW Svalbard margin) (Rasmussen et al., 2007) and atmospheric circulation (e.g. SW Barents Sea) (Risebrobakken et al., 2010).

The purpose of this study is to reconstruct the past variability of Atlantic Water influence at the western Barents Sea margin during the Holocene. We studied a sediment core retrieved from the relatively small Kveithola Trough located at the western Barents Sea margin. The trough acts as a natural sediment trap and holds 130 cm of Holocene sediments, allowing for a sampling resolution at decadal to centennial timescales (Rüther et al., 2012). The study area is located close to the present day position of the Arctic Front, below the Atlantic water masses and is therefore suitable for examining past variability of Atlantic bottom water inflow at the western Barents Sea margin.

We examined distribution patterns of benthic foraminifera faunas and benthic stable isotopes, and we quantitatively reconstructed bottom water temperatures and salinities using transfer functions.

2 Oceanographic setting

Kveithola Trough is located at the western Barents Sea margin, to the NW of Bear Island (Fig. 1). It is a 100 km long east-west trending trough, 15–20 km wide with a water depth ranging from 200 to 400 m (Rüther et al., 2012).

At present, the Barents Sea is influenced by three main water masses: Atlantic Water, Arctic Water and Coastal Water. Warm and salty Atlantic Water (> 3 °C, > 35.0 psu;

CPD
9, 4293–4322, 2013

Loeng, 1991) is transported northwards by the NAC following the continental slope of Norway (Fig. 1a). The topographically steered flow of Atlantic Water splits into two branches at ca. 72° N. One branch flows into the southern Barents Sea as the North Cape Current (NCaC) (Loeng, 1991). The other branch continues northwards along the Barents Sea slope and western Svalbard margin into the Arctic Ocean as the WSC (Aagaard et al., 1987) (Fig. 1a). The Arctic Water mass, formed by mixing of Atlantic Water and Polar Water in the Arctic Ocean, enters the Barents Sea from the north and is carried southward by the East Spitsbergen Current (ESC) and around the Svalbard archipelago (Loeng, 1991). This water mass is characterized by reduced temperatures and salinities (< 0 °C, 34.3–34.8 psu) and is seasonally covered by sea ice (Loeng, 1991). Spitsbergenbanken which encloses Kveithola Trough (Fig. 1b) is occupied by Arctic Water masses (Loeng, 1991). Transport of cold and sediment-laden shelf bottom waters from Spitsbergenbanken through Kveithola Trough to the continental slope is reported by Fohrmann et al. (1998). The boundary between Arctic and Atlantic Water is the Arctic Front (also called the Polar Front), which forms sharp climatic gradients in terms of temperature, salinity, and sea-ice distribution (Hopkins, 1991). At present, the Arctic Front is located east of our study area and south of Bear Island (Ingvaldsen, 2005). Generation of dense deep water by brine rejection primarily takes place at the Svalbard bank area and in the eastern Barents Sea (Midttun, 1985). Coastal Water is present in the southern Barents Sea and is characterized by reduced salinities (> 2 °C, < 34.7 psu; Loeng, 1991) due to freshwater runoff from the Norwegian mainland and from the Baltic Sea (Sætre, 2007).

3 Material and methods

Gravity core JM09-KA11-GC (hereafter referred to as KA11) (74°52.48′ N, 16°29.08′ E, 345 m water depth) was obtained on a cruise of R/V *Jan Mayen* in 2009 in the western part of the Kveithola Trough (Fig. 1a and b). The lithology of core KA11 was previously

CPD
9, 4293–4322, 2013

described by Rüther et al. (2012). The present study focuses on the upper 130 cm of the core.

The core was sampled continuously in 0.5 cm thick slices. All samples were weighed, freeze dried, and subsequently wet sieved using mesh sizes of 63 µm, 100 µm and 1 mm. After drying, the individual size fractions were weighed. At least 300 calcareous benthic foraminifera from the 100 µm–1 mm size fraction were picked and identified to species level, following the guidelines from Knudsen (1998). All species from the *Buccella* genus were combined and referred to as *Buccella* spp. Furthermore, the morphologically similar species *Islandiella helenae* and *Islandiella norcrossi* were combined and referred to as *Islandiella* spp. The relative abundance of the identified species was calculated in relation to all calcareous specimens per sample. Agglutinated foraminifera were nearly absent and therefore excluded from further analysis. The flux of calcareous benthic foraminifera was calculated using the dry bulk density, sedimentation rate, and number of specimens per gram dry sediment as suggested by Ehrmann and Thiede (1985):

$$\text{Flux}\,[\#\,\text{cm}^{-2}\,\text{kyr}] = [\#\,\text{g}^{-1}] \times \text{dry bulk density}\,[\text{g}\,\text{cm}^{-3}] \times \text{sedimentation rate}\,[\text{cm}\,\text{kyr}^{-1}], \quad (1)$$

where # is the number of benthic foraminiferal specimens.

Dry bulk density was calculated based on water content and wet bulk density and corrected for density of sea water.

Weight percentages of total carbon (TC), total organic carbon (TOC) and calcium carbonate ($CaCO_3$) were determined every ca. 4 cm. TC and TOC were measured at the Geological laboratory at the University of Tromsø using a LECO CS 2000 induction oven. The $CaCO_3$ content was calculated using the equation: $CaCO_3 = (TC - TOC) \times 100/12$.

Stable isotopes were measured at the Geological Mass Spectrometer (GMS) laboratory at the University of Bergen using a Finnigan 253 mass spectrometer. The reproducibility for $\delta^{18}O$ is ±0.06 ‰ and for $\delta^{13}C$ ±0.04 ‰. All stable isotope analyses were performed on *Cassidulina neoteretis*, and $\delta^{18}O$ and $\delta^{13}C$ values were corrected for

CPD
9, 4293–4322, 2013

disequilibrium with seawater by +0.02 and +1.5‰ respectively (Poole, 1994). All results are reported in ‰ VPDB. The stable oxygen isotope values were corrected for the ice-volume effect, where a sea-level change of 10 m corresponds to a 0.11 ‰ isotopic change (Fairbanks, 1989).

Thirteen radiocarbon dates were obtained using accelerator mass spectrometry (Table 1), eight dates were previously published (Rüther et al., 2012). The radiocarbon dates were measured on molluscs and monospecific samples of benthic foraminifera (Table 1). Dates from samples TRa-1066, TRa-1068 and TRa-1069 were excluded from the age model as they were obtained on infaunal mollusc species which might have migrated down in the sediment (E. Thomsen, personal communication, 2013). The radiocarbon dates were calibrated into calendar ages using Calib version 6.0 (Stuiver et al., 2005) and the marine calibration curve Marine09 (Reimer et al., 2009) with a local marine reservoir correction (ΔR) set as 67±34 (Mangerud and Gulliksen, 1975). The age model is based on linear interpolation between the remaining ten dates. The mean of the 2σ age ranges are used as tie points in the interpolation (Fig. 2). All ages in this paper are given as calibrated years BP (Present = 1950 AD).

Bottom water temperatures and salinities were reconstructed by transfer functions using the Sejrup et al. (2004) database of modern benthic foraminifera. In this database *Elphidium excavatum* f. *clavata* and *Elphidium excavatum* f. *selseyensis* are combined although they represent different temperature regimes (i.e. arctic and boreal environment; Feyling-Hanssen, 1972). In core KA11 only *E. excavatum* f. *clavata* was identified. Therefore the southernmost samples (Skagerrak, Kattegat and the Norwegian continental margin) which include *E. excavatum* f. *selseyensis*, were omitted. Additionally, three samples from fjords in Iceland were omitted since they represented a different environmental setting. Finally, *Islandiella helenae* and *Islandiella norcrossi* were combined in the database as well as the *Buccella* species. We used the C2 program (Juggings, 2010) and a weighed average partial least squares (WA-PLS) model for estimating temperature and salinity (ter Braak and Juggins, 1993). A four component WA-PLS model was used for temperature and a five component WA-PLS model for

CPD
9, 4293–4322, 2013

salinity (Table 2). This selection was based on a low root mean squared error (RMSE), the correlation between observed and estimated values (r^2), and a low maximum bias (e.g. Birks, 1995) (Table 2).

4 Results

4.1 Sedimentological parameters

The highest sedimentation rates (67 cm kyr^{-1}) are observed between 11 900–11 700 yr BP (Fig. 2). Throughout the Holocene, the sedimentation rates are much lower (4–14 cm kyr^{-1}) and generally decrease towards the present. Only during the last 1500 yr the rates increase slightly to ca. 10 cm kyr^{-1}.

The sediments consist mainly of clay and silt. Between 11 900 to 9600 yr BP the fraction < 63 µm comprises more than 90 % of the sediment, and some IRD clasts > 1 mm are observed (Fig. 3). At 9600 yr BP the sand content increases and is relatively stable until 1000 yr BP before slightly increasing again during the last 1000 yr.

The TOC percentage declines significantly from 1.7 to 0.9 wt. % at ca. 9400 yr BP and remains low, only to rise again in the last 600 yr (Fig. 3). $CaCO_3$ percentages show a slight decrease from 11 500 to 9600 yr BP, and then rise rapidly from 6 to 20 wt. %, followed by a gradual increase from 20 to 30 wt. % towards the present.

4.2 Distribution of benthic foraminifera

The benthic foraminiferal assemblage was studied at an average time resolution of 143 yr. A total of 54 species were identified. The number of species increased throughout the Holocene from around 15 to more than 30 species per sample (Fig. 3). Most specimens have well preserved tests, and no signs of dissolution were observed. Almost exclusively calcareous species were found, and the most frequent (> 5 % abundance) are shown in Fig. 4. The total flux of benthic foraminifera generally increases

CPD
9, 4293–4322, 2013

throughout the Holocene, with highest values observed between 9400–8000 yr BP and during the last 1500 yr (Fig. 3).

Three species dominate the benthic foraminiferal faunas; *E. excavatum* f. *clavata*, *Cassidulina reniforme*, and *C. neoteretis* (Fig. 4). Less frequently observed species are *Stainforthia loeblichi*, *Nonionellina labradorica*, *Islandiella* spp., *Melonis barleeanus*, *Lobatula lobatula*, and *Astrononion gallowayi*. From 11 900 to 11 700 yr BP, *S. loeblichi* and *C. reniforme* dominate the fauna with mean values of 20 and 40 % respectively. Countering the rapid decline of these two species, *E. excavatum* f. *clavata* increases till 10 500 yr BP and becomes the most abundant species with a mean value of 30 %. From 11 700 to 9400 yr BP, *C. reniforme* increases again to 40 % abundance, and *C. neoteretis* increases from 6 to 30 % abundance. During this period, *N. labradorica* and *Islandiella* spp. reach peak values of 25 and 14 % at 10 800 and 10 600 yr BP, respectively. In this same time interval, *A. gallowayi* increases to ca. 5 % abundance at 9000 yr BP and *M. barleeanus* increases to ca. 10 % at 10 000 yr BP. Both are otherwise present throughout the entire Holocene with average values of ca. 5 and 3 % respectively. From 9400 yr BP to present the benthic foraminiferal assemblage is characterized by the dominance of *C. neoteretis* and *C. reniforme* which have mean values of 27 and 34 % respectively. Some small changes are observed in the last 2000 yr when the abundance of *E. excavatum* f. *clavata* increases again, and in the last 1000 yr *M. barleeanus* increases from 2 to 6 %.

4.3 Stable isotopes

Stable isotopes are analyzed on an average time resolution of 82 yr. The δ^{18}O values are low (ca. 3.1 ‰) at 11 900 yr BP and increase rapidly to ca. 3.4 ‰ at 11 700 yr BP (Fig. 5). From 11 700 to 10 500 yr BP the δ^{18}O values are stable at 3.4 ‰. The δ^{18}O values fluctuate between 10 500–9000 yr BP after which they show a relatively stable, slightly increasing trend, with an average value of 3.7 ‰ throughout the rest of the Holocene.

CPD
9, 4293–4322, 2013

The $\delta^{13}C$ values decrease from 0.8 to 0.4 ‰ between 11 900 and 8800 yr BP. From 8800 to 7000 yr BP, $\delta^{13}C$ values increase by 0.4 ‰ after which they remain relatively stable till ca. 1500 yr BP. Over the last 1500 yr $\delta^{13}C$ values increase to 1 ‰.

4.4 Bottom water temperatures and salinities

Bottom water temperatures estimated by transfer functions increase from 0.7 to 3.2 °C between 11 900 and 9600 yr BP (Fig. 5). This increase, however, is punctuated by a brief cold interval with temperatures less than 1 °C at ca. 10 700 yr BP. The last 9600 yr show relatively stable temperatures with an average value of 3.2 °C ±0.4. The reconstructed salinity values exhibit a similar trend as the bottom water temperatures (Fig. 5) and increase from 34.7 to 34.9 psu between 11 600 to 10 000 yr BP. After 10 000 yr BP the salinity is stable at 34.9 psu ± 0.03.

5 Paleoceanographic development at the western Barents Sea margin and regional correlation

We divide our Holocene record into four time slices: Younger Dryas–Holocene transition (11 900–11 700 yr BP), Early Holocene (11 700–9400 yr BP), Mid Holocene (9400–1500 yr BP), and Late Holocene (1500 yr BP–present). These subdivisions are based on changes in the benthic foraminiferal fauna, stable oxygen isotopes, and grain-size distribution. Boundaries are placed at midpoints of changes.

5.1 Younger Dryas–Holocene transition (11 900–11 700 yr BP)

During the transition period from the Younger Dryas to the Holocene, the total benthic foraminiferal flux is rather low (Fig. 3), indicating unfavorable environmental conditions at the study site. This could be caused by the relatively high sedimentation rates and enhanced IRD production (Figs. 2 and 3), which reflects increased sediment transport by icebergs and/or sea-ice. Concordantly, depleted $\delta^{18}O$ values and the relatively low

CPD
9, 4293–4322, 2013

salinity values (Fig. 5) suggest a freshwater input. Unfavorable environmental conditions are further supported by the rapid increase of the opportunistic species *E. excavatum* f. *clavata* which replaces *S. loeblichi*, a species associated with seasonal sea-ice and pulses of seasonal high productivity (Steinsund, 1994; Polyak et al., 2002), and the glacio-marine indicator *C. reniforme* (e.g. Polyak et al., 2002) (Fig. 4). The presence of *E. excavatum* f. *clavata* most likely reflects an environment with more extensive sea-ice cover, high turbidity, and lowered fluctuating salinities (Steinsund, 1994; Hald et al., 1994; Hald and Korsun, 1997). We therefore infer that the benthic foraminiferal assemblage reflects predominantly polar conditions with associated meltwater input. Rüther et al. (2012) report that since the deglaciation of Kveithola Trough (14 200 yr BP) a semi-perennial sea-ice cover persisted. The timing of the deglaciation of the surrounding Spitsbergenbanken is not well constrained but a minimum deglaciation age of 11 200 yr BP has been inferred for Bear Island (Wohlfarth et al., 1995). Meltwater from the glaciers located at Bear Island during the Younger Dryas will have been partly discharged through Kveithola Trough since its inner basin is connected to channels which drain parts of the Bear Island banks (Fohrmann et al., 1998). While the trough was still influenced by meltwater input and presence of sea ice, bottom water temperatures started to rise (Fig. 5), indicating an enhanced advection of Atlantic Water to the western Barents Sea margin. This development corresponds to a regional pattern in the Barents Sea area with warm Atlantic Water influencing the bottom waters at the end of the Younger Dryas (Rasmussen et al., 2007, 2012; Aagaard-Sørensen et al., 2010; Skirbekk et al., 2010).

5.2 Early Holocene (11 700–9400 yr BP)

During the Early Holocene significant changes occurred in the foraminiferal fauna, which was still scarce but became more diverse (Fig. 3). Initially, the benthic fauna was dominated by *E. excavatum* f. *clavata* and *C. reniforme*, indicating cold conditions with lowered salinities and possibly high water turbidity (Hald et al., 1994; Steinsund, 1994; Hald and Korsun, 1997). The subsequent decrease of *E. excavatum* f. *clavata* and

CPD
9, 4293–4322, 2013

increase in temperature and salinity values (Fig. 5) suggests an overall improvement of environmental conditions reflecting the continued increasing influence of Atlantic Water. This is further corroborated by the increase of *C. neoteretis* and *M. barleeanus* which are both associated with chilled Atlantic Water in the Arctic (Mackensen and Hald, 1988; Steinsund, 1994; Seidenkrantz, 1995). Furthermore, the increase of *N. labradorica* also supports an increased influence of Atlantic Water since this species is linked to the higher nutrient content of Atlantic derived waters and oceanic fronts (Hald and Korsun, 1997; Rytter et al., 2002; Jennings et al., 2004; Lloyd, 2006). The pulse of *Islandiella* spp. shortly after the increase of *N. labradorica* points to a seasonal sea-ice cover and/or close proximity to the sea-ice margin (Hald and Steinsund, 1996). The presence of periodic sea-ice cover is further supported by the low total flux (Fig. 3), indicating unfavorable conditions at the sea floor. A submerged inflow of Atlantic Water beneath the sea-ice would develop a stratified water column, which tends to limit biological productivity (Stein and Macdonald, 2004). The pulses of *N. labradorica* and *Islandiella* spp. indicate unstable environmental conditions and the presence of sea-ice/proximity of the Arctic Front at the western Barents Sea margin 74° N. These findings are similar to those of Risebrobakken et al. (2010).

The increase of Atlantic Water associated species from ca. 11 000 yr BP towards the present contradicts the decline of bottom water temperatures for this time. Between 11 000 and 10 500 yr BP, temperatures show a decline of more than 1.5 °C (Fig. 5) despite the increasing influence of warm Atlantic Water. The δ^{18}O values are stable in this interval (Fig. 5). They only show a change of 0.15 ‰ (Fig. 5), whereas a temperature change of 1.5 °C would correspond to a change in δ^{18}O of 0.4 ‰ (Shackleton, 1974). The offset between the δ^{18}O values and the bottom water temperatures calculated with transfer functions could be due to the different seasonal signal that these records represent. The transfer functions reflect average summer temperature (July, August, September; Sejrup et al., 2004) whereas the δ^{18}O value measured on *C. neoteretis* might reflect a different season. Hald et al. (2011) for instance report that for Malangen fjord *C. neoteretis* may calcify in late autumn. In addition, comparing the low

CPD
9, 4293–4322, 2013

temperatures with the foraminiferal abundance, we find that these points correlate with high abundances of *N. labradorica* and *Islandiella* spp. (Fig. 4). Both species are associated with high productivity environments (Hald and Steinsund, 1996; Polyak et al., 2002), and *N. labradorica* is controlled more by food supply than by water temperature (Hald and Korsun, 1997; Lloyd, 2006; Ivanova et al., 2008). Hence, the temperature decline is likely overestimated due to the training set.

Reconstructed salinities show an increase at 11 600 yr BP pointing to an enhanced influence of Atlantic Water (Fig. 5). This inference is further supported by the gradual increase of *M. barleeanus,* an Arctic-Boreal species which prefers higher salinities (Hald and Steinsund, 1992; Jennings et al., 2004) and is associated with the presence of Atlantic derived waters in the Artic (Polyak et al., 2002). The increase of *M. barleeanus* is also concurrent with the high TOC content and the high percentage of fine-grained sediments (Fig. 3). *M. barleeanus* is reported to feed on organic detritus which can be delivered with fine sediments from shallow areas and then deposited in local depocenters (Polyak et al., 2002). We therefore speculate that the rapid decrease of TOC content at 9400 yr BP, corresponding with changes observed in sedimentation rate and grain size, most likely represents a regime change of the bottom currents whereby the supply of fine-grained sediments and organic material from the shallow bank areas enclosing Kveithola Trough ceased. Winnowing is not an uncommon feature in the Early Holocene in the region although in the southern Barents Sea it ceased 700 yr later at 8700 yr BP due to eustatic sea-level rise (Hald and Vorren, 1984). The ceased winnowing at Kveithola Trough might be explained by a lowered influence of Arctic Water occupying the shallow banks to the N and NE and a stronger inflow of Atlantic Water.

A stronger inflow of Atlantic Water in the Early Holocene is also evident from several records from the Svalbard and Barents Sea region (e.g. Duplessy et al., 2005; Ślubowska-Woldengen et al., 2007; Chistyakova et al., 2010; Rasmussen et al., 2012; Klitgaard Kristensen et al., 2013). The strong inflow of Atlantic Water is associated with peak Holocene temperatures as observed by transfer function generated bottom water temperatures (Rasmussen et al., 2013), benthic foraminiferal assemblages (Ślubowska

CPD
9, 4293–4322, 2013

et al., 2005; Skirbekk et al., 2010), and benthic oxygen isotopes (Risebrobakken et al., 2010) at the western and northern Svalbard shelf and SW Barents Sea. However, in the present records we do not observe Early Holocene peak temperatures in the $\delta^{18}O$ record nor in the benthic foraminiferal assemblages. This Early Holocene climate optimum is widely recognized in marine and terrestrial records from the Nordic Seas region. It is considered as a response to the Early Holocene orbital forcing (Renssen et al., 2009), resulting in higher-than-present summer insolation in the Northern Hemisphere (Berger and Loutre, 1991) (Fig. 5), and as response to a stronger inflow of Atlantic Water and the resulting heat advection northward (Hald et al., 2007; Risebrobakken et al., 2011). The lack of the Early Holocene warming optimum in the bottom waters of Kveithola Trough is consistent with a study by Risebrobakken et al. (2011). They show that ocean temperatures underneath the summer mixed layer in the eastern Nordic Seas do not increase significantly at this time and must instead be representative of the mean state of Atlantic Water inflow. Additionally, at the time of maximum heat transport through the NAC (around 10 000 yr BP; Risebrobakken et al., 2011) the study site was still influenced by Arctic Water, thereby possibly suppressing the warming signal.

5.3 Mid Holocene (9400–1500 yr BP)

The Mid Holocene is characterized by a stable benthic faunal distribution which is dominated by two species, *C. neoteretis* and *C. reniforme*. Together they comprise more than 60 % of the fauna. This indicates a consistent influence of Atlantic Water throughout the Mid Holocene which has increased compared to the Early Holocene. Further, the stable values of $CaCO_3$ content (wt. %) and the increased total benthic foraminiferal flux, imply a more productive, stable environment due to the strengthened and constant inflow of Atlantic Water.

Increasing $\delta^{18}O$ values throughout the Mid Holocene imply a decrease in temperature or an increase in salinity. The $\delta^{18}O$ values follow the decreasing insolation at 70° N (Fig. 5) (Berger and Loutre, 1991) suggesting the $\delta^{18}O$ values indicate a cooling

CPD
9, 4293–4322, 2013

trend. However, this cooling trend is not observed in the reconstructed bottom water temperatures (Fig. 5); either because the two records represent a different seasonal signal or the temperature decrease is too small to influence the benthic faunal distribution. If we assume the $\delta^{18}O$ signal is only controlled by temperature this would correspond to a temperature decline of > 1.5 °C (Shackleton, 1974) from the Mid Holocene to present. Thereby the temperature decline is consistent with decreasing bottom water temperatures in the Barents Sea region as recorded by distribution patterns of benthic foraminifera and benthic $\delta^{18}O$ values (e.g. Husum and Hald, 2004; Ślubowska-Woldengen et al., 2007; Rasmussen et al., 2012). In addition, the temperature trend for the bottom waters are consistent with the decreasing surface water temperatures as recorded by planktic foraminifera and diatoms in the Nordic Seas (e.g. Sarnthein et al., 2003; Andersen et al., 2004). The stable climatic conditions and the slight gradual cooling that we observe is also concurrent with findings from the SW Barents Sea (Chistyakova et al., 2010; Risebrobakken et al., 2010).

5.4 Late Holocene (1500 yr BP–present)

Throughout the last 1500 yr more unstable conditions are observed compared to the Mid Holocene. The coarse grain-size fraction has increased, episodes of enhanced productivity are suggested by peak values in foraminiferal concentration, and small changes in the species composition and abundances occur (Figs. 3 and 4). The coarser grain-size fraction suggests a more vigorous current regime probably due to a stronger inflow of Atlantic Water at the western Barents Sea margin. This is also observed in a sortable silt record from the Yermak Plateau (Hass, 2002). Further, an increased inflow of Atlantic Water is observed along the western and northern margins of the Barents Sea and Svalbard (Lubinski et al., 2001; Ślubowska et al., 2005; Jernas et al., 2013; Dylmer et al., 2013) thereby indicating a regional enhanced inflow of Atlantic Water.

The episodes of enhanced productivity suggest a higher availability of nutrients. We observe an increase in the abundance of *M. barleeanus*, pointing to a change in food

CPD
9, 4293–4322, 2013

availability (Polyak et al., 2002), and an increase in TOC content. At the same time, a biomarker analysis on core KA11 shows that the study site is again influenced by seasonal sea-ice in the Late Holocene (Berben et al., 2013). Also, a stronger mixing of the water column is suggested by the higher δ^{13}C values. The fluxes of *E. excavatum* f. *clavata* reach the same level as during the Early Holocene, although with a much lower relative abundance (< 5 %). Apparently, conditions are becoming more favorable for this species which could indicate periodically colder conditions or a higher turbidity of the water column (Steinsund, 1994; Hald et al., 1994; Hald and Korsun, 1997). However, colder conditions are not observed in the δ^{18}O values or in the reconstructed bottom water temperatures (Fig. 5). The changes that are observed in productivity, foraminiferal abundance, and sea-ice presence might suggest that an oceanographic front, associated with sea-ice and higher productivity, is moving towards our core location. This implies that there is an overall stronger inflow of Atlantic water in Kveithola Trough which is interrupted by periods of reduced inflow and subsequently colder conditions.

The changing bottom water conditions as observed by the benthic foraminiferal fauna are also observed in several other benthic foraminiferal records in the Barents Sea and Svalbard region (Ślubowska et al., 2005; Ślubowska-Woldengen et al., 2007; Chistyakova et al., 2010; Risebrobakken et al., 2010; Rasmussen et al., 2012; Jernas et al., 2013) although timing of the onset differs between the regions. Similar to the observations from Kveithola Trough, unstable bottom water conditions are observed along the western Svalbard margin (Ślubowska-Woldengen et al., 2007) due to episodic inflow of Atlantic Water (Rasmussen et al., 2012).

At Kveithola Trough the temperatures remain stable from Mid- to Late Holocene. Hereby core KA11 differs from others records from the Barents Sea and western Svalbard margin which do observe a temperature change. Several records record a cooling in the Late Holocene in both the bottom (Ślubowska-Woldengen et al., 2007; Risebrobakken et al., 2010) and surface water masses (Voronina et al., 2001; Hald et al., 2007; Rasmussen et al., 2007; Risebrobakken et al., 2010) which could be related to

CPD
9, 4293–4322, 2013

declining summer insolation (Berger and Loutre, 1991) or displacements of Arctic and Polar Water masses (Hald et al., 2007). Opposite to this cooling, two high-resolution studies from Bear Island (Wilson et al., 2011) and the western and northern Svalbard shelf (Jernas et al., 2013) infer a warming over the last ~ 200 yr induced by the renewed influence of Atlantic Water. In Kveithola Trough we do not observe a temperature increase over the last few hundred years which may be due to loss of the uppermost sediment during the coring procedure.

In conclusion, the Late Holocene, as recorded in core KA11, underwent frequently changing environmental conditions as is also observed in the SW Barents Sea (Risebrobakken et al., 2010) and in marine and terrestrial environments in the Nordic Seas region (e.g. Nesje et al., 2005).

6 Conclusions

A sediment core from the western Barents Sea margin was analyzed with regard to benthic foraminiferal assemblages and stable isotopes on high resolution in order to elucidate past variability of Atlantic bottom water during the Holocene. Further, bottom water temperatures and salinities were reconstructed with transfer functions.

Our results show that Atlantic Water has been continuously present at the western Barents Sea margin throughout the studied interval. The transition from the Younger Dryas to the Holocene occurred between 11 900 and 11 700 yr BP and is characterized by glaciomarine conditions with extensive sea-ice cover and meltwater input as suggested by low δ^{18}O and salinity values. During the Early Holocene the influence of Atlantic Water increased although sea-ice was still present in Kveithola Trough; however, bottom waters experienced a rapid warming whereby the predominantly polar benthic foraminiferal fauna was replaced by a subpolar fauna. The following transition to the Mid Holocene is characterized by a local shift in current regime through which we speculate that the supply of fine material from the shallow bank areas surrounding Kveithola Trough ceased. The Mid Holocene (9400–1500 yr BP) was a stable

CPD
9, 4293–4322, 2013

climatic period with favorable environmental conditions and throughout this time there was a consistent inflow of Atlantic Water. Bottom water temperatures declined during the Mid Holocene, thereby following the insolation curve at 70° N. During the last 1500 yr the inflow of Atlantic Water increased as observed from the coarser grain-size fraction. However, climatic conditions also became more unstable which may be related to periods of increased influence of Arctic Water that caused periodically colder conditions.

Acknowledgements. This work is a contribution to the CASE Initial Training Network funded by the European Community's 7th Framework Programme FP7 2007/2013, Marie-Curie Actions, under Grant Agreement No. 238 111. Additional funding was provided by the Norwegian Research Council. We thank Denise Rüther for sharing data from core JM09-KA11-GC and Edel Ellingsen for picking foraminifera for AMS dates. We also thank Jan P. Holm for providing the maps for Fig. 1 and Andrew James Smith for correcting the English language.

References

Aagaard, K. and Greisman, P.: Toward new mass and heat budgets for the Arctic Ocean, J. Geophys. Res., 80, 3821–3827, doi:10.1029/JC080i027p03821, 1975.

Aagaard, K., Foldvik, A., and Hillman, S. R.: The West Spitsbergen current: disposition and water mass transformation, J. Geophys. Res., 92, 3778–3784, doi:10.1029/JC092iC04p03778, 1987.

Aagaard-Sørensen, S., Husum, K., Hald, M., and Knies, J.: Paleoceanographic development in the SW Barents Sea during the Late Weichselian–Early Holocene transition, Quaternary Sci. Rev., 29, 3442–3456, doi:10.1016/j.quascirev.2010.08.014, 2010.

Andersen, C., Koç, N., Jennings, A., and Andrews, J. T.: Nonuniform response of the major surface currents in the Nordic Seas to insolation forcing: implications for the Holocene climate variability, Paleoceanography, 19, PA2003, doi:10.1029/2002pa000873, 2004.

Berben, S. M. P., Husum, K., Cabedo Sanz, P., and Belt, S. T.: Holocene sub centennial evolution of Atlantic water inflow and sea ice distribution in the western Barents Sea, Clim. Past, submitted, 2013.

CPD
9, 4293–4322, 2013

Berger, A. and Loutre, M.: Insolation values for the climate of the last 10 million years, Quaternary Sci. Rev., 10, 297–317, doi:10.1016/0277-3791(91)90033-Q, 1991.
Birks, H. J. B.: Quantitative paleoenvironmental reconstructions, in: Statistical Modelling of Quaternary Science Data, edited by: Maddy, D. and Brew, J. S., Quaternary Research Association, Cambridge, UK, 116–254, 1995.
Chistyakova, N., Ivanova, E., Risebrobakken, B., Ovsepyan, E., and Ovsepyan, Y.: Reconstruction of the postglacial environments in the southwestern Barents Sea based on foraminiferal assemblages, Oceanology, 50, 573–581, doi:10.1134/S0001437010040132, 2010.
Duplessy, J. C., Ivanova, E., Murdmaa, I., Paterne, M., and Labeyrie, L.: Holocene paleoceanography of the northern Barents Sea and variations of the northward heat transport by the Atlantic Ocean, Boreas, 30, 2–16, doi:10.1111/j.1502-3885.2001.tb00984.x, 2001.
Duplessy, J. C., Cortijo, E., Ivanova, E., Khusid, T., Labeyrie, L., Levitan, M., Murdmaa, I., and Paterne, M.: Paleoceanography of the Barents Sea during the Holocene, Paleoceanography, 20, PA4004, doi:10.1029/2004PA001116, 2005.
Dylmer, C. V., Giraudeau, J., Eynaud, F., Husum, K., and De Vernal, A.: Northward advection of Atlantic water in the eastern Nordic Seas over the last 3000 yr, Clim. Past, 9, 1505–1518, doi:10.5194/cp-9-1505-2013, 2013.
Ehrmann, W. U. and Thiede, J.: History of Mesozoic and Cenozoic sediment fluxes to the North Atlantic Ocean, Contrib. Sedimentol., 15, 1–109, 1985.
Fairbanks, R. G.: A 17 000-year glacio-eustatic sea level record: influence of glacial melting rates on the Younger Dryas event and deep-ocean circulation, Nature, 342, 637–642, 1989.
Feyling-Hanssen, R. W.: The Foraminifer Elphidium excavatum (Terquem) and its variant forms, Micropaleontology, 18, 337–354, 1972.
Fohrmann, H., Backhaus, J. O., Blaume, F., and Rumohr, J.: Sediments in bottom-arrested gravity plumes: numerical case studies, J. Phys. Oceanogr., 28, 2250–2274, 1998.
Hald, M. and Korsun, S.: Distribution of modern benthic foraminifera from fjords of Svalbard, European Arctic, J. Foramin. Res., 27, 101–122, doi:10.2113/gsjfr.27.2.101, 1997.
Hald, M. and Steinsund, P. I.: Distribution of surface sediment benthic foraminifera in the southwestern Barents Sea, J. Foramin. Res., 22, 347–362, doi:10.2113/gsjfr.22.4.347, 1992.
Hald, M. and Steinsund, P. I.: Benthic foraminifera and carbonate dissolution in the surface sediments of the Barents and Kara Seas, Ber. Polarforsch., 212, 285–307, 1996.
Hald, M. and Vorren, T. O.: Modern and Holocene foraminifera and sediments on the continental shelf off Troms, North Norway, Boreas, 13, 133–154, 1984.

CPD
9, 4293–4322, 2013

Hald, M., Steinsund, P. I., Dokken, T., Korsun, S., Polyak, L., and Aspeli, R.: Recent and late Quaternary distribution of Elphidium excavatum f. clavatum in the Arctic seas, Cushman Foundation Special Publications, 32, 141–153, 1994.

Hald, M., Andersson, C., Ebbesen, H., Jansen, E., Klitgaard-Kristensen, D., Risebrobakken, B., Salomonsen, G. R., Sarnthein, M., Sejrup, H. P., and Telford, R. J.: Variations in temperature and extent of Atlantic Water in the northern North Atlantic during the Holocene, Quaternary Sci. Rev., 26, 3423–3440, doi:10.1016/j.quascirev.2007.10.005, 2007.

Hald, M., Salomonsen, G. R., Husum, K., and Wilson, L. J.: A 2000 year record of Atlantic Water temperature variability from the Malangen Fjord, northeastern North Atlantic, Holocene, 21, 1049–1059, doi:10.1177/0959683611400457, 2011.

Hass, H. C.: A method to reduce the influence of ice-rafted debris on a grain size record from northern Fram Strait, Arctic Ocean, Polar Res., 21, 299–306, doi:10.1111/j.1751-8369.2002.tb00084.x, 2002.

Hopkins, T. S.: The GIN Sea – a synthesis of its physical oceanography and literature review 1972–1985, Earth-Sci. Rev., 30, 175–318, doi:10.1016/0012-8252(91)90001-v, 1991.

Husum, K. and Hald, M.: A continuous marine record 8000–1600 cal. yr BP from the Malangen-fjord, north Norway: foraminiferal and isotopic evidence, Holocene, 14, 877–887, 2004.

Ingvaldsen, R. B.: Width of the North Cape Current and location of the Polar Front in the western Barents Sea, Geophys. Res. Lett., 32, L16603, doi:10.1029/2005gl023440, 2005.

Ivanova, E. V., Ovsepyan, E. A., Risebrobakken, B., and Vetrov, A. A.: Downcore distribution of living calcareous foraminifera and stable isotopes in the western Barents Sea, J. Foramin. Res., 38, 337–356, 2008.

Jennings, A. E., Weiner, N. J., Helgadottir, G., and Andrews, J. T.: Modern foraminiferal faunas of the southwestern to northern Iceland shelf: oceanography and environmental controls, J. Foramin. Res., 34, 180–207, doi:10.2113/34.3.180, 2004.

Jernas, P., Klitgaard Kristensen, D., Husum, K., Wilson, L., and Koç, N.: Paleoenvironmental changes of the last two millennia on the western and northern Svalbard shelf, Boreas, 42, 236–255, 2013.

Klitgaard-Kristensen, D., Sejrup, H. P., and Haflidason, H.: The last 18 kyr fluctuations in Norwegian sea surface conditions and implications for the magnitude of climatic change: evidence from the North Sea, Paleoceanography, 16, 455–467, doi:10.1029/1999PA000495, 2001.

CPD
9, 4293–4322, 2013

Klitgaard Kristensen, D., Rasmussen, T. L., and Koč, N.: Palaeoceanographic changes in the northern Barents Sea during the last 16 000 years – new constraints on the last deglaciation of the Svalbard–Barents Sea Ice Sheet, Boreas, 42, 798–813, doi:10.1111/j.1502-3885.2012.00307.x, 2013.

Knudsen, K. L.: Foraminiferer I Kvartær stratigrafi: Laboratorie og fremstillingsteknik samt udvalgte eksempler, Geologisk Tidsskrift, 3, 1–25, 1998.

Lloyd, J. M.: Modern distribution of benthic foraminifera from Disko Bugt, West Greenland, J. Foramin. Res., 36, 315–331, 2006.

Loeng, H.: Features of the physical oceanographic conditions of the Barents Sea, Polar Res., 10, 5–18, doi:10.1111/j.1751-8369.1991.tb00630.x, 1991.

Lubinski, D. J., Polyak, L., and Forman, S. L.: Freshwater and Atlantic water inflows to the deep northern Barents and Kara seas since ca 13 ^{14}C ka: foraminifera and stable isotopes, Quaternary Sci. Rev., 20, 1851–1879, doi:10.1016/S0277-3791(01)00016-6, 2001.

Mackensen, A. and Hald, M.: Cassidulina teretis Tappan and C. laevigata d'Orbigny; their modern and late Quaternary distribution in northern seas, J. Foramin. Res., 18, 16–24, doi:10.2113/gsjfr.18.1.16, 1988.

Mangerud, J. and Gulliksen, S.: Apparent radiocarbon ages of recent marine shells from Norway, Spitsbergen, and Arctic Canada, Quaternary Res., 5, 263–273, doi:10.1016/0033-5894(75)90028-9, 1975.

Midttun, L.: Formation of dense bottom water in the Barents Sea, Deep-Sea Res. Pt. 1, 32, 1233–1241, 1985.

Nesje, A., Jansen, E., Birks, J. B., Bjune, A. E., Bakke, J., Andersson Dahl, C., Dahl, S. O., Klitgaard Kristensen, D., Lauritzen, S. E., Lie, Ø., Løvlie, R., Risebrobakken, B., and Svendsen, J. I.: Holocene climate variability in the North Atlantic region: a review of marine and terrestrial evidence, in: The Nordic seas, an integrated perspective, edited by: Drange, H., Dokken, T., Furevik, T., Gerdes, R., and Berger, W. H., AGU Geophysical Monograph, 289–322, 2005.

Polyak, L., Korsun, S., Febo, L. A., Stanovoy, V., Khusid, T., Hald, M., Paulsen, B. E., and Lubinski, D. J.: Benthic foraminiferal assemblages from the southern Kara Sea, a river-influenced arctic marine environment, J. Foramin. Res., 32, 252–273, doi:10.2113/32.3.252, 2002.

Poole, D.: Neogene and Quaternary Paleoenvironments in the Norwegian Sea Shelf, Ph.D Thesis, University of Tromsø, Tromsø, Norway, 1994.

CPD
9, 4293–4322, 2013

Rasmussen, T. L., Thomsen, E., Ślubowska, M. A., Jessen, S., Solheim, A., and Koç, N.: Paleoceanographic evolution of the SW Svalbard margin (76° N) since 20,000 ^{14}C yr BP, Quaternary Res., 67, 100–114, doi:10.1016/j.yqres.2006.07.002, 2007.

Rasmussen, T. L., Forwick, M., and Mackensen, A.: Reconstruction of Atlantic Water to Isfjorden, Svalbard during the Holocene: correlation to climate and seasonality, Mar. Micropaleontol., 94–95, 80–90, 2012.

Rasmussen, T. L., Thomsen, E., Skirbekk, K., Slubowska-Woldengen, M., Klitgaard Kristensen, D., and Koç, N.: Holocene temperature variability in the northern Nordic Seas: interplay of Atlantic-, Arctic- and Polar water masses, Quaternary Sci. Rev., submitted, 2013.

Reimer, P. J., Baillie, M. G. L., Bard, E., Bayliss, A., Beck, J. W., Blackwell, P. G., Ramsey, C. B., Buck, C. E., Burr, G. S., Edwards, R. L., Friedrich, M., Grootes, P. M., Guilderson, T. P., Hajdas, I., Heaton, T. J., Hogg, A. G., Hughen, K. A., Kaiser, K. F., Kromer, B., McCormac, F. G., Manning, S. W., Reimer, R. W., Richards, D. A., Southon, J. R., Talamo, S., Turney, C. S. M., van der Plicht, J., and Weyhenmeye, C. E.: IntCal09 and Marine09 radiocarbon age calibration curves, 0–50,000 yr cal BP, Radiocarbon, 51, 1111–1150, 2009.

Renssen, H., Seppä, H., Heiri, O., Roche, D. M., Goosse, H., and Fichefet, T.: The spatial and temporal complexity of the Holocene thermal maximum, Nat. Geosci, 2, 411–414, doi:10.1038/ngeo513, 2009.

Risebrobakken, B., Jansen, E., Andersson, C., Mjelde, E., and Hevrøy, K.: A high-resolution study of Holocene paleoclimatic and paleoceanographic changes in the Nordic Seas, Paleoceanography, 18, 1017, doi:10.1029/2002PA000764, 2003.

Risebrobakken, B., Moros, M., Ivanova, E. V., Chistyakova, N., and Rosenberg, R.: Climate and oceanographic variability in the SW Barents Sea during the Holocene, Holocene, 20, 609–621, doi:10.1177/0959683609356586, 2010.

Risebrobakken, B., Dokken, T., Smedsrud, L., Andersson, C., Jansen, E., Moros, M., and Ivanova, E.: Early Holocene temperature variability in the Nordic Seas: the role of oceanic heat advection versus changes in orbital forcing, Paleoceanography, 26, PA4206, doi:10.1029/2011PA002117, 2011.

Rüther, D. C., Bjarnadóttir, L. R., Junttila, J., Husum, K., Rasmussen, T. L., Lucchi, R. G., and Andreassen, K.: Pattern and timing of the northwestern Barents Sea Ice Sheet deglaciation and indications of episodic Holocene deposition, Boreas, 41, 494–512, doi:10.1111/j.1502-3885.2011.00244.x, 2012.

CPD
9, 4293–4322, 2013

Rytter, F., Knudsen, K. L., Seidenkrantz, M. S., and Eiríksson, J.: Modern distribution of benthic foraminifera on the north Icelandic shelf and slope, J. Foramin. Res., 32, 217–244, doi:10.2113/32.3.217, 2002.

Sætre, R.: The Norwegian coastal current: oceanography and climate, Tapir Academic Press, Trondheim, 2007.

Sarnthein, M., Van Kreveld, S., Erlenkeuser, H., Grootes, P. M., Kucera, M., Pflaumann, U., and Schulz, M.: Centennial-to-millennial-scale periodicities of Holocene climate and sediment injections off the western Barents shelf, 75° N, Boreas, 32, 447–461, doi:10.1111/j.1502-3885.2003.tb01227.x, 2003.

Seidenkrantz, M. S.: Cassidulina teretis Tappan and Cassidulina neoteretis new species (Foraminifera): stratigraphic markers for deep sea and outer shelf areas, J. Micropalaeontol., 14, 145–157, doi:10.1144/jm.14.2.145, 1995.

Sejrup, H. P., Birks, H. J. B., Klitgaard Kristensen, D., and Madsen, H.: Benthonic foraminiferal distributions and quantitative transfer functions for the northwest European continental margin, Mar. Micropaleontol., 53, 197–226, doi:10.1016/j.marmicro.2004.05.009, 2004.

Shackleton, N. J.: Attainment of isotopic equilibrium between ocean water and the benthonic foraminifera genus Uvigerina: isotopic changes in the ocean during the last glacial, Centre National de la Recherche Scientifique Colleagues Internationeaux, 219, 203–209, 1974.

Skirbekk, K., Klitgaard Kristensen, D., Rasmussen, T. L., Koç, N., and Forwick, M.: Holocene climate variations at the entrance to a warm Arctic fjord: evidence from Kongsfjorden trough, Svalbard, in: Fjord Systems and Archives, edited by: Howe, J. A., Austin, W. E. N., Forwick, M., and Paetzel, M., Special Publications, 344, Geological Society of London, London, 289–304, 2010.

Ślubowska, M. A., Koç, N., Rasmussen, T. L., and Klitgaard-Kristensen, D.: Changes in the flow of Atlantic water into the Arctic Ocean since the last deglaciation: evidence from the northern Svalbard continental margin, 80° N, Paleoceanography, 20, PA4014, doi:10.1029/2005PA001141, 2005.

Ślubowska-Woldengen, M., Rasmussen, T. L., Koç, N., Klitgaard-Kristensen, D., Nilsen, F., and Solheim, A.: Advection of Atlantic Water to the western and northern Svalbard shelf since 17500 cal yr BP, Quaternary Sci. Rev., 26, 463–478, doi:10.1016/j.quascirev.2006.09.009, 2007.

Stein, R. and Macdonald, R. W.: The Organic Carbon Cycle in the Arctic Ocean, Springer, Berlin, 2004.

CPD
9, 4293–4322, 2013

Steinsund, P. I.: Benthic foraminifera in surface sediments of the Barents and Kara Seas: Modern and Late Quaternary Applications, Ph.D thesis, University of Tromsø, Tromsø, Norway, 1994.
Stuiver, M., Reimer, P. J., and Reimer, R. W.: CALIB 6.0, WWW program and documentation, 2005.
ter Braak, C. J. F. and Juggins, S.: Weighted averaging partial least squares regression (WA-PLS): an improved method for reconstructing environmental variables from species assemblages, Hydrobiologia, 269–270, 485–502, doi:10.1007/bf00028046, 1993.
Voronina, E., Polyak, L., De Vernal, A., and Peyron, O.: Holocene variations of sea-surface conditions in the southeastern Barents Sea, reconstructed from dinoflagellate cyst assemblages, J. Quaternary Sci., 16, 717–726, doi:10.1002/jqs.650, 2001.
Wilson, L. J., Hald, M., and Godtliebsen, F.: Foraminiferal faunal evidence of twentieth-century Barents Sea warming, Holocene, 21, 527–537, doi:10.1177/0959683610385718, 2011.
Wohlfarth, B., Lemdahl, G., Olsson, S., Persson, T., Snowball, I., Ising, J., and Jones, V.: Early Holocene environment on Bjørnøya (Svalbard) inferred from multidisciplinary lake sediment studies, Polar Res., 14, 253–275, 1995.

CPD
9, 4293–4322, 2013

Table 1. AMS ^{14}C dates and calibrated dates for core JM09-KA11-GC. The dates were dated at; TRa: Radiocarbon Laboratory in Trondheim, Norway and Uppsala, Sweden and Beta: Beta Analytic Inc. in Miami, Florida, US. Radiocarbon ages are calibrated in the Calib 6.0 programme (Stuiver and Reimer, 1993) using the Marine09 calibration curve (Reimer et al., 2009). A standard reservoir correction of 400 yr and regional ΔR value of 67 ± 34 (Mangerud and Gulliksen, 1975) were used. Dates marked with * from Rüther et al. (2012).

Lab reference	Core level (cm)	Dated material	^{14}C date	Calibrated age	Calibrated age range ±2σ	δ^{13}C (‰)	Comments
TRa-1063	3–6	*Bathyarca glacialis*-unpaired	925 ± 30*	476	396–555	2.3	
TRa-1064	3–6	*Bathyarca glacialis*-unpaired	900 ± 35*	444	352–536 334–344	4.5	
TRa-1065	15–17	*Bathyarca glacialis*	1880 ± 35*	1375	1268–1482	4.4	
Beta-324049	27.5–28	*Islandiella norcorssi/helenae*	4430 ± 30	4518	4383–4653 4663–4675	−1.5	
TRa-1066	32.5–33.5	*Astarte elliptica*-unpaired	1990 ± 35*	1469	1345–1593	5.5	not used
Beta-315192	39.5–40.5	*Islandiella norcorssi/helenae*	5480 ± 30	5779	5665–5893	−1.3	
Beta-315193	44–45	*Islandiella norcorssi/helenae*	6510 ± 40	6943	6783–7103	−1.9	
TRa-1067	53–57	*Astarte sulcata*-unpaired	7630 ± 45*	8038	7920–8155	5.7	
Beta-315194	80–81	*Islandiella norcorssi/helenae*	8770 ± 40	9367	9249–9485	−2.6	
TRa-1068	81–83.5	*Astarte elliptica*-paired	8140 ± 50*	8545	8389–8701	3.6	not used
TRa-1069	81–83.5	*Nucunala minuta*-unpaired	8315 ± 50*	8783	8597–8968	4.7	not used
Beta-315195	110.5–111.5	*Elphidium excavatum f. clavata*	10 540 ± 50	11 612	11 324–11 899	−2.8	
TRa-1070	133–136	*Yoldiella intermedia*-paired	10 705 ± 55*	11 964	11 676–12 252	3.3	

CPD
9, 4293–4322, 2013

Table 2. Performance of transfer function model WA-PLS with components 1 to 5. In bold performance of the selected models.

Model	Temperature			Salinity		
	RMSE	r^2	Max bias	RMSE	r^2	Max bias
WA-PLS component 1	1.24877	0.748377	2.34502	0.106815	0.561906	0.573909
WA-PLS component 2	1.12137	0.797089	1.72035	0.0978157	0.632613	0.472159
WA-PLS component 3	1.03408	0.827448	1.27498	0.0923698	0.672383	0.399328
WA-PLS component 4	**0.996462**	**0.839779**	**1.0828**	0.0894319	0.692892	0.407719
WA-PLS component 5	0.973128	0.847195	1.14311	**0.0858414**	**0.717062**	**0.395228**

CPD
9, 4293–4322, 2013

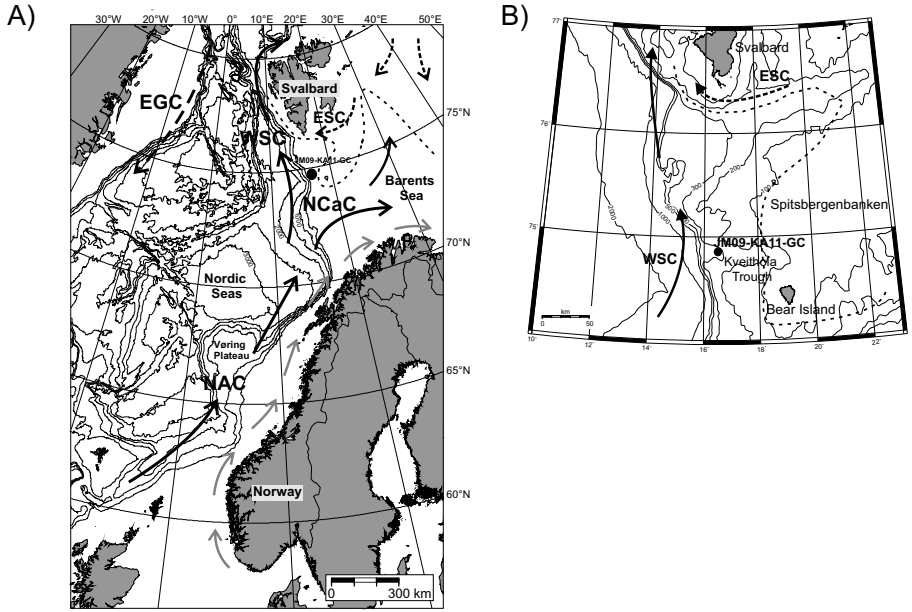

Fig. 1. (A) Location of study site JM09-KA11-GC together with main surface current systems in the region. Dashed line indicates the present day position of the Polar Front (after Loeng, 1991). Black currents indicate Atlantic Water, grey currents indicate Coastal Water, dashed black currents indicate Arctic Water. Abbreviations are NAC, North Atlantic Current; NCaC, North Cape Current; WSC, West Spitsbergen Current; ESC, East Spitsbergen Current; EGC, East Greenland Current. **(B)** Detail map of study area showing location of studied core.

CPD
9, 4293–4322, 2013

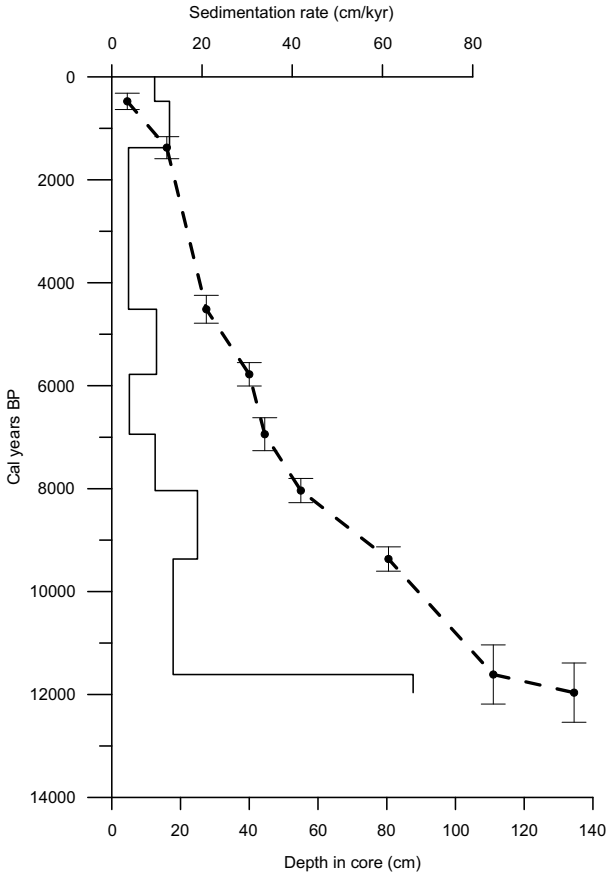

Fig. 2. Age model and sedimentation rate of JM09-KA11-GC. The 2σ ranges are indicated on the dated levels. Chronology is established by linear interpolation between calibrated ages.

CPD
9, 4293–4322, 2013

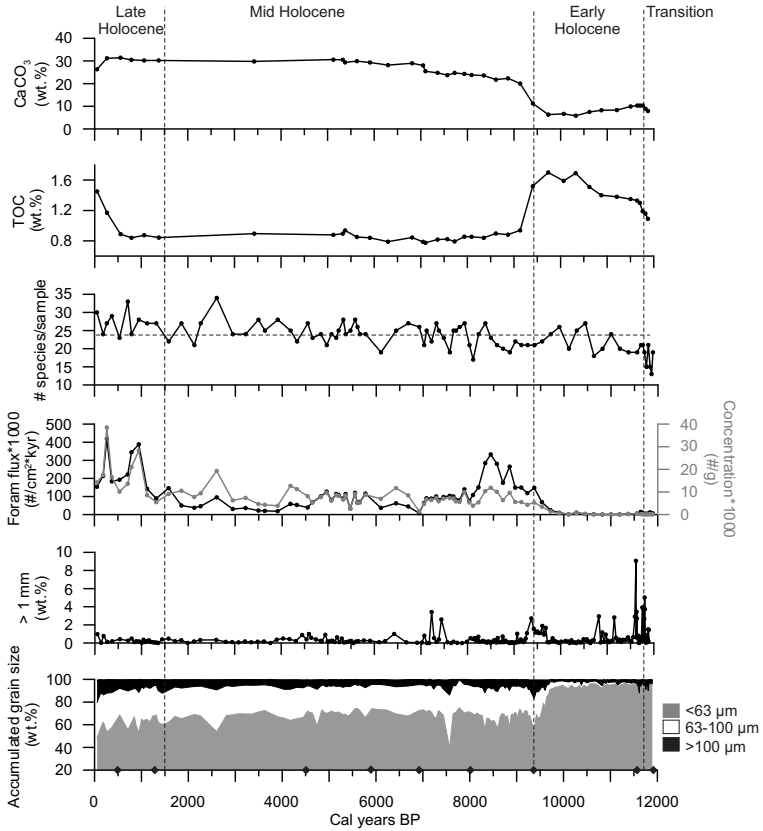

Fig. 3. Sediment properties of core JM09-KA11-GC. Accumulated grain size as weight percentage, number of benthic species per sample with dashed line indicating average value, benthic foraminiferal flux together with foraminiferal concentration, TOC and $CaCO_3$ as weight percentage. The size fraction > 1 mm is considered as ice rafted debris (IRD). Black diamonds on *x* axis indicate AMS ^{14}C dates.

CPD
9, 4293–4322, 2013

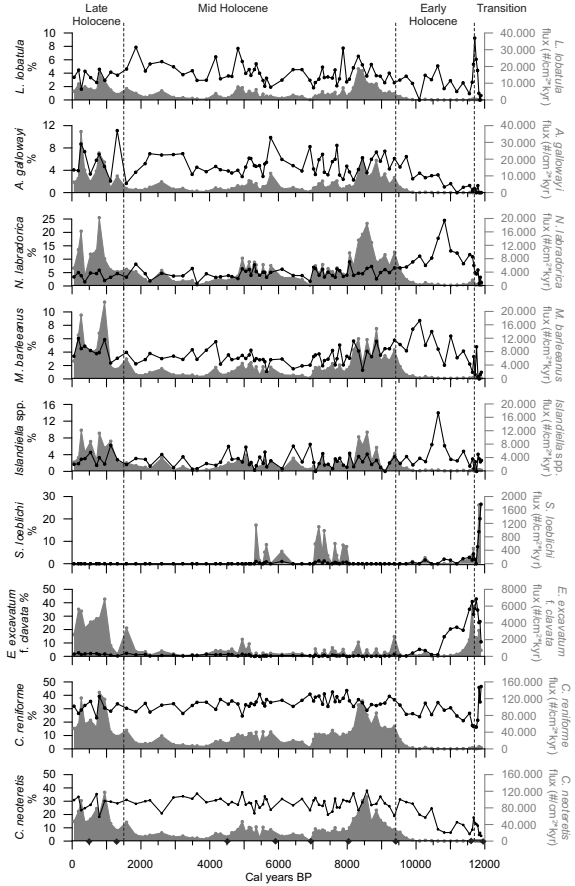

Fig. 4. Relative abundances (left, black) and fluxes (right, grey shading) of the most frequent benthic foraminiferal species versus calendar age BP. Note the different scales. Black diamonds on *x* axis indicate AMS ^{14}C dates.

CPD
9, 4293–4322, 2013

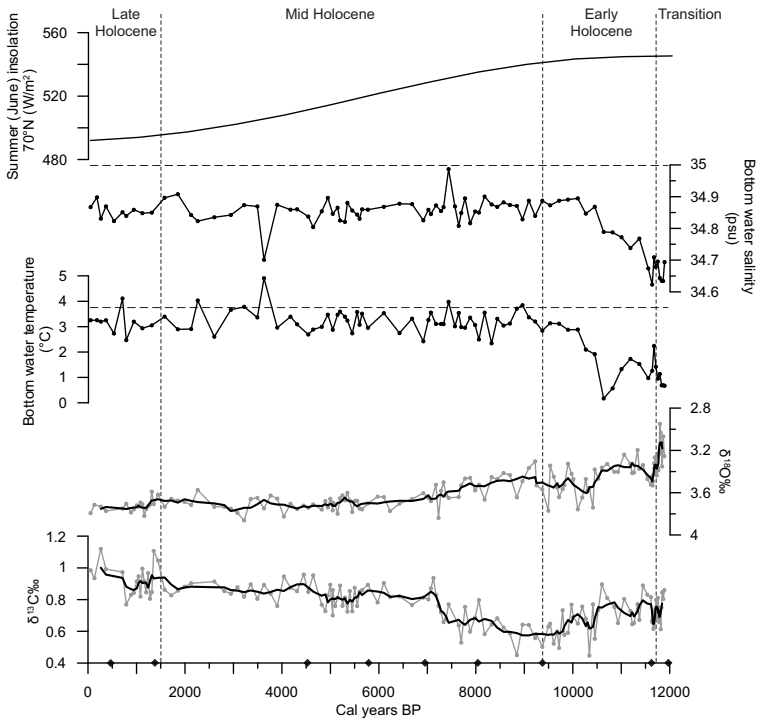

Fig. 5. Stable isotope records (grey lines) with 5 point running average (black lines) shown together with temperature and salinity records calculated by transfer functions for core JM09-KA11-GC. $\delta^{18}O$ values are corrected for global ice-volume and both stable isotope records are corrected for disequilibrium effects. Present day temperature and salinity values are indicated by dashed lines. Top graph showing June insolation at 70° N (Berger and Loutre, 1991). Black diamonds on *x* axis indicate AMS ^{14}C dates.

CPD
9, 4293–4322, 2013